Response Surface Methodology-Assisted Optimization, Purification, Characterization and Application of Natural Dye from *Bischofia Javanica* Leaves on Cotton

Poro D. Clark[1,*]

[1]Department of Chemistry, Federal University of Petroleum Resources, Effurun, Nigeria

*Corresponding author email: clark.poro@fupre.edu.ng

Received: Dec 12, 2025 **Revised**: Jun 04, 2026 **Just Accepted Online**: Jun 17, 2026 **Published**: Xxx

Please cite this article as:
P.D. Clark (2026) Response Surface Methodology-Assisted Optimization, Purification, Characterization and Application of Natural Dye from *Bischofia Javanica* Leaves on Cotton. **Substantia**. *Just Accepted*. DOI: 10.36253/Substantia-3883

Abstract:
This study optimized the extraction of natural dyes from *Bischofia javanica* Blume leaves using a Soxhlet apparatus, with process conditions determined by response surface methodology and a central composite design (RSM-CCD). The effects of extraction temperature (46–74 °C) and time (0.6–3.4 h) were investigated over 14 experimental runs. Extraction efficiency, quantified by measuring absorbance at 430 nm using UV-Vis spectrophotometry, was maximized at optimized conditions of approximately 70 °C for 2 hours, yielding a threefold increase in absorbance compared to lower temperatures. The main dye fraction (F3) was purified and isolated using gravity column chromatography on silica gel and confirmed by TLC. The dyed cotton fabric was evaluated for its physical fastness properties (light, wash, perspiration, and rubbing). Characterization techniques, including UV-Vis, FTIR, and HPLC, identified isoquercetin as the primary dye compound along with berberine and eugenol, confirming that the extract is rich in flavonoids. At an 8% dye concentration, cotton treated with potassium aluminum sulfate mordant showed higher color strength (K/S) and exhibited excellent light fastness (grade 6–7), very good wash fastness (rating 4), and dry rubbing fastness (rating 4). Perspiration fastness was better under acidic conditions (3-4) due to stable aluminum-flavonoid complexes, which enhanced photostability and wash resistance compared to unmordanted fabric. This study demonstrates that *Bischofia javanica* leaves are a promising source of natural dyes for sustainable textiles and highlights how statistical optimization can significantly improve extraction efficiency, supporting potential eco-friendly industrial applications.

Key words: *Bischofia javanica*, Natural dye, Central composite design, Isoquercetin, Flavonoids, Color fastness

1. INTRODUCTION

Natural dyes extracted from plants are gaining renewed scientific and industrial interest due to the growing environmental concerns surrounding synthetic colorants [1]. Conventional dyes derived from petroleum, commonly used in the textile industry, are associated with persistent water pollution, poor biodegradability, and documented toxicological risks, such as allergenicity and carcinogenicity [2]. While many studies have suggested that plant-based dyes could serve as safer alternatives, their wider adoption has been constrained by issues related to extraction efficiency, color consistency, and scalability. As a result, there is an urgent need for systematic research that not only identifies promising botanical sources but also optimizes their extraction and application parameters.

Bischofia javanica Blume (bishop wood or toog tree), a tropical species native to Southeast Asia and the Pacific Islands, presents such promise but remains largely unexplored as a dye source. Traditionally used for medicinal, flavoring, and wood applications, its leaves are known to contain substantial amounts of polyphenols, flavonoids,

tannins, and other compounds, such as betulinic acid, friedelin, luteolin, and quercetin, which are widely reported as chromogenic and antibacterial agents in successful natural dye systems [3,4]. The bark and leaves yield natural brown to black dyes rich in tannins commonly used for fabric decoration in some cultures. Moreover, extracts exhibit antimicrobial activity, enhancing the functional value of the dye for textile applications. While a recent study by Risnasari *et al*. [5] demonstrated the antibacterial and dye potential of *B. javanica* in eco-printing, this preliminary investigation highlighted the need for more rigorous research, since insufficient attention has been given thus far to optimizing extraction conditions, purification, or rigorous evaluation of dyeing performance on textile fibers such as cotton. Their study, however, pursued a fundamentally different approach: it characterized the leaf and twig biomass primarily by pyrolysis gas chromatography–mass spectrometry, emphasized its lignin and polyphenol content, and fixed the color through an eco-printing technique using a range of mordants (alum, ferrous sulfate, and sodium acetate). It neither optimized the solvent extraction variables, isolated the principal chromophore, nor quantified the conventional fastness properties of the resulting dyeings. The present work therefore complements and extends that report by coupling statistically optimized Soxhlet extraction with chromatographic purification, structural identification of the dominant flavonoid, and comprehensive fastness evaluation on a single, well-defined fiber.

.

The extraction of natural dyes often faces challenges such as low yields and variability due to insufficiently controlled process parameters like temperature, solvent composition, and time. Soxhlet extraction remains one of the most reliable methods for the exhaustive recovery of polar phytochemicals. However, its successful application depends heavily on the optimization of operating parameters. Statistical approaches such as Response Surface Methodology (RSM), particularly Central Composite Design (CCD), offer a powerful means to determine the interactive effects between variables, minimize trial numbers, and generate predictive models for process intensification [6]. While RSM has been widely applied to various dye plants, this methodology has yet to be utilized for *B. javanica*.

Equally crucial is the establishment of their chemical identity and application performance of the extracted dyes. UV-visible spectrophotometry provides rapid assessment of chromophoric strength, while Fourier Transform Infrared (FTIR) spectroscopy enables identification of functional groups responsible for dye-fiber binding [7,8]. High-performance liquid chromatography (HPLC) affords deeper insight into dye composition and purity, supporting reproducibility and potential industrial transferability [9]. Cotton, a cellulosic fiber rich in hydroxyl groups, serves as a model substrate to assess dyeability owing to its affinity for phenolic and tannin-based colorants via hydrogen bonding interactions [10].

Therefore, this study aimed to advance the foundation of previous work by systematically optimizing dye extraction from *B. javanica* leaves using Soxhlet-assisted RSM-CCD, coupled with purification procedures, comprehensive spectroscopic and chromatographic characterization, and subsequent application on cotton fabric. his approach rigorously addresses extraction efficiency, dye quality, and fiber–dye interaction, ultimately establishing *B. javanica* as a viable and scalable natural dye source that contributes to the sustainable coloration of textiles with multifunctional benefits.

2. MATERIALS AND METHODS

2.1 Materials

Fresh leaves of *B. javanica* were obtained from a cultivated plot in Otu-Jeremi, Delta State, Nigeria. The specimen underwent taxonomic verification by the Botanical Survey Unit at the University of Calabar, Nigeria, where a voucher sample (Reference No.: 2024/CAL/HRB222) was deposited for future reference. Analytical-grade potassium aluminum sulfate (alum; Batch No.: ALM/KAT/04-24/NG) was procured from Katchey Company Limited (Ikeja, Lagos). Additional reagents, such as sodium carbonate (Na_2CO_3), sodium chloride (NaCl), acetic acid (CH_3COOH), ethanol (C_2H_5OH), sodium hydroxide (NaOH), chloroform ($CHCl_3$), methanol (CH_3OH), and a non-ionic detergent solution, and distilled water (Batch No.: CHEM/JMK/09-23/LG), were sourced from Jemok Nigeria Limited in Egbeda, Lagos. These were utilized as scouring agents, pH adjusters, solvents, and exhausting aids during fabric pretreatment and dyeing processes. A 100% pure cotton fabric (Batch No.: WF/LOT/02-24) served as the dye substrate for dyeing. All batch numbers were recorded to ensure traceability of materials and to facilitate the reproducibility of experimental results.

2.2 Instruments

A Soxhlet extractor (BES-402, Behr Labor-Technik, Germany) coupled with a heating mantle (EM0500/E, Electothermal, UK) was used for extraction. Sample weighing was performed using a precision balance (FA2104A, Gulfex). UV-visible measurements were conducted using a Shimadzu UV-1800 spectrophotometer

(Japan). Fractionation was performed using a silica gel column (Silica Gel 60, Merck, Germany). Fourier transform infrared (FTIR) spectra were recorded using a Shimadzu IRTracer-100 spectrometer (Japan), while high-performance liquid chromatography (HPLC) analysis was performed on an Agilent 1260 Infinity II system (USA). Color fastness evaluations were conducted using a washing fastness tester (Chiuvention), crockmeter (Gester), rubbing fastness tester (GT-D05), and perspirometer (TF416A, TESTEX).

2.3 Optimization design of experiment (DOE)

The extraction of *Bishofia javanica* leaves using ethanol was optimized using a central composite design (CCD). This two-factor and five-level CCD included 14 experimental runs to assess and model the impact of process variables on extraction efficiency. Temperature (X_1) and extraction time (X_2) were chosen as the independent variables, with their coded and actual levels presented in Table 1. An empirical second-order polynomial model (Equation 1) was used to describe the behavior of the system. The regression coefficients for the model were estimated from experimental data.

$$Y = \beta_0 + \beta_1 X_1 + \beta_2 X_2 + \beta_{11} X^2_1 + \beta_{22} X^2_2 + \beta_{12} X_1 X_2 \quad (1)$$

In this equation, Y represents the response variable (the absorbance of the extract), β_o is the intercept, while β_1 and β_2 are the linear coefficients. The quadratic coefficients are denoted by β_{11} and β_{22} with β_{12} reflecting the interaction effect between temperature and time. All experimental trials were performed in triplicate and statistical evaluation of the model was conducted using Design Expert software 13.

Table 1. Experimental parameters and their corresponding coded levels

Parameter	Symbol	Coded levels					Mean	Standard deviation
		-α	**-1**	**0**	**+1**	**+α**		
Temperature (°C)	X_1	45.86579	50	60	70	74.1421	60.00	0.7845
Extraction time (hr)	X_2	0.5858	1	2	3	3.4142	2.00	7.84

2.4 Extraction of dye

The Soxhlet extraction procedure was adapted from that described by Otutu *et al.* [11] and Clark *et al.* [12], with the key modification being the use of a central composite design (CCD) to optimize the parameters. Ten (10) grams of powdered *B. javanica* leaves were loaded into a cellulose extraction thimble (size 33 mm × 94 mm) and placed in the extraction chamber of the Soxhlet apparatus. Extraction was carried out with 200 ml of 95% ethanol, giving a solvent to solid ratio of 20:1 (mL/g). A thermostatically controlled heating mantle was used to maintain the extraction temperature. The independent variables, temperature (X_1, 50-70 °C) and time (X_2, 1-3 h) were set according to the experimental matrix defined by the CCD (Table 1). After each extraction cycle, the resulting crude filtrates were analyzed using a UV-Vis spectrophotometer, with the absorbance measured at 430 nm to determine the extraction yield.

The extract yielding the highest absorbance was selected as the most efficient and was subsequently purified via silica gel gravity column chromatography and further characterized using FTIR, HPLC, and UV-Vis scanning spectrophotometry.

2.5 Column chromatography

Purification was performed using gravity column chromatography, as described in the literature [10]. A total of 1.20 g of the crude ethanol extract was loaded onto a column packed with 160 g of silica gel. The sample was eluted using a gradient of chloroform and methanol, with increasing polarity, to optimize the separation. A total of 88 fractions (25 mL each) were collected and analyzed by thin-layer chromatography (TLC). Based on the TLC profiles, the fractions were pooled into five combined fractions (F1-F5): F1 (fractions 1-20), F2 (21-36), F3 (37-55), F4 (56-71), and F5 (72-88). Fraction F3, which showed a single dominant spot on TLC (Rf = 0.65), was

identified as the main, high-purity dye fraction and was subsequently selected for structural elucidation by UV-Vis, FTIR, and HPLC.

2.6 Phytochemical screening tests

Phytochemical screening was performed on the chromatographic fraction of *B. javanica* leaves using standard colorimetric tests [13-15]. The tests targeted alkaloids, flavonoids, terpenoids, tannins, saponins, and cardiac glycosides. The results were recorded as positive (+) or negative (−) based on the color changes observed.

2.7 Dyeing procedures

The dyeing process followed the general method described by Clark and Ekpekpo [10], with modifications to incorporate fabric pre-treatment, alum mordanting, and graded dye concentrations. Prior to dyeing, the fabric samples were scoured in an alkaline bath containing 2 g/L sodium carbonate and 1 g/L non-ionic detergent at 60-70 °C for 30 minutes to remove impurities and residual finishing agents. The fabrics were then rinsed thoroughly with distilled water and air-dried.

Mordanting was carried out using potassium aluminum sulfate [KAl(SO4)2] at 2-8% o.w.f. (on weight of fabric). The fabrics were immersed in the mordant solution at a liquor ratio of 1:10 and heated to 80-90 °C for 30-45 min. After treatment, the samples were rinsed with distilled water and lightly squeezed. Unmordanted samples were reserved and dyed directly without prior treatment. Dyeing was conducted on both the mordanted and unmordanted fabrics. Aqueous dye solutions were prepared at four individual concentrations: 2%, 4%, 6%, and 8% (w/v), each maintained at a liquor ratio of 1:10. The pH of the dye bath was adjusted according to the dye source; for *Bischofia javanica*, alkaline conditions (pH 9-10) were achieved by dropwise addition of 0.1 M sodium hydroxide, while acidic conditions (pH 3-4) were obtained using 0.1 M hydrochloric acid. The temperature of the dye bath was increased gradually at approximately 1 °C/min until it reached 100 °C and maintained for 60 minutes. After dyeing, the bath was allowed to cool to approximately 60 °C before the fabric was removed. Excess liquor was expelled by squeezing, followed by thorough rinsing with distilled water. The dyed fabrics were air-dried under ambient laboratory conditions.

2.8 Determination of color fastness

The washing fastness of the dyed fabrics was evaluated using the 105-C10:2006 standard method [16]. The fabrics were washed with a soap solution for 30 min at 60 °C, and the extent of staining on adjacent undyed fabrics was assessed by comparing them with the grey scale (1-5). For the measurement of light fastness, the samples were exposed to sunlight for 72 hours in accordance with the ISO 105-B01:2014 standard [17]. The degree of fading (change in color) was assessed by comparing them with the blue scale standard (1-8). The dry and wet rubbing fastness of the dyed samples was determined according to the standard technique, ISO 105-X12:2001 [18]. The color fastness to perspiration was determined according to the ISO 105-EO4 standard method [19]. Two perspiration solutions (acidic and alkaline) were prepared by dissolving 0.5 g histidine monohydrochloride monohydrate, sodium dihydrogen orthophosphate dihydrate (2.2 g), and 5.0 g of sodium chloride in 1 L of distilled water. The pH was adjusted to 5.5 by adding 0.1 N NaOH. The alkaline medium was prepared by mixing 5 gL^{-1} NaCl, 2.5 gL^{-1} $Na_2HPO_2.2H_2O$, and 0.5 gL^{-1} $C_6H_9O_2{}^-N_3$. $HCl.H_2O$. The solution was adjusted to a pH of 8.0 with 0.1 N NaOH using a liquor ratio of 20:1. The composite samples (7.5 x 6.5 cm) were placed in a perspirometer at 37±2 °C. After 4 hours, the composite samples were removed from the perspirometer and dried at room temperature (25 °C). The change in color and staining of the adjacent white fabrics was assessed using the grey scale standard (1-5)

.

2.9 Color measurement

The CIE L^*, a^*, and b^* color coordinates for the dyed samples were measured using a colorimeter. In this regard, L^* is the brightness, a^* is the extent of redness (if +ve), or greenness (if –ve), and b^* is the extent of yellowness (if +ve) or blueness (if –ve).

The strength of the dyed samples was expressed as K/S and was measured using the light reflectance method. The K/S values were calculated using the Kubelka–Munk equation (Equation 1).

$K/S = (I - R)^2 / 2R$ (1)

Where R refers to the reflectance, K represents the absorption coefficient and S is the light scattering coefficient.

3. RESULTS AND DISCUSSION

3.1 Influence of process variables (temperature and time) on extraction performance

The extraction process was optimized using a central composite design (CCD) to evaluate the combined effects of extraction time (0.6–3.4 h) and temperature (46–74.1 °C) on absorbance at 430 nm, which served as a measure of extraction efficiency (Table 2). The absorbance values showed significant variation across experimental runs (0.21–0.66 AU), demonstrating a 3.1-fold difference between the least and most effective conditions, confirming that the extraction performance is highly sensitive to the process parameters.

Temperature proved to be the primary factor influencing extraction efficiency. At a consistent duration of 2 hrs, increasing temperature from 46 °C to 74.1 °C enhanced absorbance nearly threefold (0.26 to 0.66 AU), while a similar trend was observed at 1 hr, where increasing temperature from 50 °C to 70 °C raised absorbance from 0.21 to 0.59 AU. High-temperature conditions (70-74 °C) consistently yielded higher responses (0.57-0.66 AU), regardless of extended extraction time, suggesting that equilibrium in extraction is reached rapidly at elevated temperatures. This strong dependence on temperature indicates that factors such as solvent penetration, solute solubility, and mass transfer kinetics are driven by thermal conditions within this system.

The pronounced relationship between extraction efficiency and temperature is consistent with previous studies on the solvent extraction of plant pigments and phenolic compounds, where different temperatures (50, 60, 70, or 80 °C) under stirring conditions showed that higher temperatures resulted in greater diffusivities and increased amounts of extracted bioactive compounds [19]. Researchers have also pointed out that higher temperatures can enhance solubility and diffusion during extraction; however, it is essential to avoid excessive heat, as overheating can lead to solvent loss and degradation of phenolic compounds [20].

The rapid attainment of extraction equilibrium observed at 70-74 °C aligns with reports indicating that diffusion coefficients and equilibrium properties are assessed during solid–liquid extraction, with the amount of extracted bioactive compounds at equilibrium varying significantly with temperature [19]. This suggests that extending the extraction time beyond equilibrium may not significantly improve yield but could increase solvent usage or risk thermal degradation of heat-sensitive compounds. Moreover, the marked variability in absorbance values across experimental runs highlights the sensitivity of bioactive compound extraction to operational parameters. Carpentieri *et al.* [21] emphasized this in their study on process optimization using response surface methodology and central composite design. Their research demonstrated that response surface methodology enables insights into how various processing variables interact with target response variables while minimizing the number of experimental runs.

In contrast, extraction time exerted a secondary yet temperature-dependent influence, a trend consistent with previous findings in studies on natural pigment and phytochemical extractions. Many studies have indicated that extraction efficiency varies with time within a certain range until equilibrium is reached for the solute inside and outside the solid material [22]. The slight improvements observed at 60 °C and minimal gains beyond 1 h at 70 °C support the findings that high temperatures can lead to thermal degradation of polyphenols; this mechanism often explains reductions in polyphenol yield during high-temperature extractions, as prolonged exposure can damage heat-sensitive compounds [23]. However, the notable increase in absorbance over time at lower temperatures, such as 50 °C, corroborates findings from response surface methodology studies investigating extraction parameters at 60-80 °C and times of 80–120 min, which showed that insufficient thermal energy at lower temperatures necessitates longer extraction periods to achieve comparable yields [19]. This time-dependent compensation effect is typical of extractions influenced by diffusion-controlled kinetics, where higher temperatures can increase solubility and diffusion, with thermal energy affecting both the rate of mass transfer and the accessibility of bound compounds within plant matrices [24].

Table 2. Central composite design matrix and experimental responses for extraction optimization of *B. javanica* leaves

Std	Run	Factor 1 A: Time (hr)	Factor 2 B: Temperature (°C)	Response 1 Absorbance (AU)
7	1	2	46	0.26
8	2	2	74.1	0.66
3	3	1	70	0.59
13	4	2	60	0.38
9	5	2	60	0.44
1	6	1	50	0.21
14	7	2	60	0.41
4	8	3	70	0.57
5	9	0.6	60	0.31
6	10	3.4	60	0.51
11	11	2	60	0.36
2	12	3	50	0.47
12	13	2	60	0.42
10	14	2	60	0.39

The ANOVA results for the quadratic model (Table 3) show that the model was highly significant ($F = 48.67$, $p < 0.0001$), affirming that the relationship between the independent variables (time and temperature) and the response (absorbance) was statistically reliable. The small residual mean square (0.0008) and high F-value indicate an excellent fit of the model to the experimental data, demonstrating that the variation in absorbance was primarily explained by the fitted equation rather than by random error.

Among the model terms, temperature (B) exerted the most significant effect ($F = 165.75$, $p < 0.0001$), followed by time (A) ($F = 41.44$, $p = 0.0002$). The interaction term (AB) was also statistically significant ($F = 23.77$, $p = 0.0012$), confirming that the effect of extraction time depended on the temperature level. This supports the contour and 3D surface plots, where time had a stronger influence at lower temperatures but was less important under high-temperature conditions.

The quadratic term for temperature (B^2) was significant ($F = 11.77$, $p = 0.0090$), indicating a curvature effect in the response surface, which defines the existence of a true optimum within the studied range, rather than a simple linear trend. Conversely, the quadratic term for time (A^2) was not significant ($p = 0.3181$), suggesting that the extraction time affects the absorbance mainly in a linear manner without substantial curvature.

The lack-of-fit test was not significant ($p = 0.4829$*), demonstrating that the model adequately fits the experimental data and that the unexplained variation was due to pure error rather than model inadequacy. This, coupled with the

small residual error and good reproducibility of the center points (CV = 7.5%), confirms the reliability and predictive strength of the quadratic model.

Table 3. ANOVA results for quadratic model on time and temperature effects in *B. javanica* leaves

Source	Sum of Squares	Df	Mean Square	F-value	p-value	
Model	0.2007	5	0.0401	48.67	< 0.0001	Significant
A-Time	0.0342	1	0.0342	41.44	0.0002	
B-Temperature	0.1367	1	0.1367	165.75	< 0.0001	
AB	0.0196	1	0.0196	23.77	0.0012	
A^2	0.0009	1	0.0009	1.13	0.3181	
B^2	0.0097	1	0.0097	11.77	0.0090	
Residual	0.0066	8	0.0008			
Lack of Fit	0.0024	3	0.0008	0.9513	0.4829	not significant
Pure Error	0.0042	5	0.0008			
Cor Total	0.2073	13				

Diagnostic statistics were examined to evaluate the adequacy of the quadratic model for absorbance prediction. The close agreement between the actual and predicted absorbance values (Table 4) indicates that the model accurately describes the experimental data, with small residuals across most runs. The residuals ranged from 0.028 to +0.040, demonstrating minimal deviation between observed and fitted values, thereby confirming good model fit.

The internally and externally studentized residuals were generally within the acceptable range of ±2, suggesting that no data point exerted undue influence on model estimation. Two runs (1 and 6) showed slightly higher externally studentized residuals (-1.77 and +1.86, respectively), but both remained below the critical threshold of ±3, indicating that they were not true outliers. These points correspond to the lowest and highest temperature conditions (46 °C and 74 °C), where natural variability in extraction yield is expected due to the thermal sensitivity of the pigments.

The Cook's distance values were all below 1.0, further confirming the absence of influential observations that could distort the regression coefficients. Similarly, leverage values ranged between 0.167 and 0.625, within the recommended limits for CCD models, suggesting a balanced influence of design points across the experimental space. The DFFITS values, used to measure the influence on the fitted response, were below the cutoff of ±2 for all runs except two marginal cases (runs 1 and 6), which again correspond to boundary points rather than statistical anomalies. These diagnostic statistics collectively validate that the model is robust, stable, and free from significant outliers or influential data points. The random distribution of residuals around zero (not systematic) and the low residual variance (0.0008) further indicate that the model predictions are unbiased and statistically sound.

Table 4. Diagnostic statistics for model adequacy evaluation in the extraction study of *B. javanica* leaves

Run Order	Actual Value	Predicted Value	Residual	Leverage	Internally Studentized Residuals	Externally Studentized Residuals	Cook's Distance	Influence on Fitted Value DFFITS	Standard Order
1	0.2600	0.2876	-0.0276	0.625	-1.572	-1.769	0.687	-2.284[1]	7
2	0.6600	0.6574	0.0026	0.625	0.151	0.141	0.006	0.182	8
3	0.5900	0.5829	0.0071	0.625	0.406	0.384	0.046	0.496	3
4	0.3800	0.4000	-0.0200	0.167	-0.763	-0.741	0.019	-0.331	13
5	0.4400	0.4000	0.0400	0.167	1.526	1.695	0.078	0.758	9
6	0.2100	0.1814	0.0286	0.625	1.624	1.856	0.733	2.396[1]	1
7	0.4100	0.4000	0.0100	0.167	0.381	0.360	0.005	0.161	14
8	0.5700	0.5736	-0.0036	0.625	-0.203	-0.190	0.011	-0.246	4
9	0.3100	0.3301	-0.0201	0.625	-1.141	-1.167	0.362	-1.507	5
10	0.5100	0.5149	-0.0049	0.625	-0.280	-0.263	0.022	-0.340	6
11	0.3600	0.4000	-0.0400	0.167	-1.526	-1.695	0.078	-0.758	11
12	0.4700	0.4521	0.0179	0.625	1.015	1.018	0.286	1.314	2
13	0.4200	0.4000	0.0200	0.167	0.763	0.741	0.019	0.331	12
14	0.3900	0.4000	-0.0100	0.167	-0.381	-0.360	0.005	-0.161	10

The contour plot illustrates the combined effects of temperature (B) and time (A) on absorbance, which reflects the extraction efficiency of the dye from *B. javanica* leaves (Table 4). The color gradient from blue to yellow indicates a progressive increase in absorbance from 0.21 to 0.66 AU, corresponding to low and high extraction efficiencies.

A clear trend is observed where the absorbance increases sharply with temperature, particularly beyond 65 °C, confirming that temperature is the dominant factor influencing pigment release. The steep gradient along the temperature axis, compared to the relatively gentle gradient along the time axis, signifies that increasing temperature exerts a far stronger positive effect than extending extraction time, consistent with findings showing that contour plots reveal the different values of the response depending on various combinations of variables, with temperature generally showing stronger effects on extraction efficiency [21]. This trend is consistent with diffusion-controlled extraction kinetics, where higher temperatures enhance solvent penetration, solute solubility, and mass transfer rates, thereby accelerating pigment release into the solvent phase [19].

At moderate temperatures (55–60 °C), the contour lines were more widely spaced, suggesting a synergistic interaction between time and temperature. In this region, extending extraction time from 1 h to 3 h moderately improved absorbance, indicating that longer extraction durations can partly compensate for reduced thermal energy input, consistent with response surface analysis showing that both temperature and time significantly influence extraction yield, although with different magnitudes of effect [23]. However, at elevated temperatures (≥ 70 °C), the contour lines became nearly horizontal, reflecting diminishing returns from time extension, a point at which extraction equilibrium is reached rapidly, and further time offers little or no improvement in yield due to

solvent saturation [24].

The predicted optimum region lies near the upper boundary of the design space, at approximately 70 °C and 2 h, where the absorbance values approach 0.66 AU. This agrees with the statistical output of the CCD model, confirming that maximum dye recovery occurs under high-temperature and moderate-time conditions, with response surface methodology enabling the visualization of optimal conditions through three-dimensional surface graphs and contour plots. The clustering of design points along this region and the narrow variance among replicates indicate excellent model reproducibility and predictive reliability.

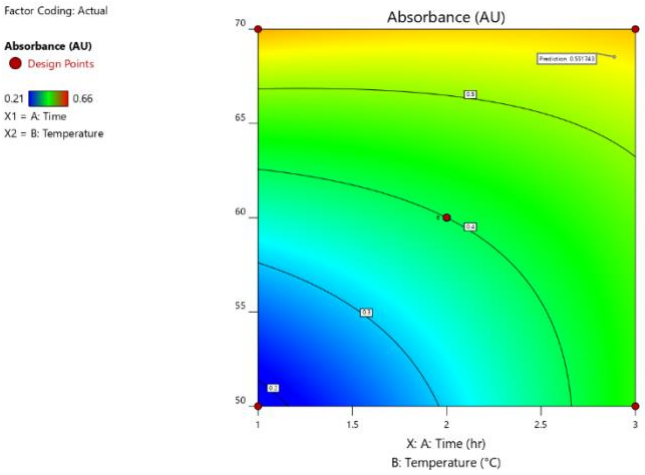

Figure 1. 2D Contour plot showing the effect of time and temperature on absorbance

The three-dimensional (3D) surface plot offers a detailed visualization of how extraction temperature (B) and time (A) together influence absorbance at 430 nm, indicating dye extraction efficiency from *B. javanica* leaves (Figure 1). The curved surface illustrates how the response changes across the design space, with a color gradient from blue (low absorbance, approximately 0.21 AU) to yellow (high absorbance, approximately 0.66 AU). The surface shows a clear upward curvature along the temperature axis, confirming that temperature is the main factor affecting extraction performance. As temperature increases from 50 °C to 70 °C, absorbance increases sharply, reflecting better pigment solubility, improved solvent diffusivity, and faster mass transfer. This aligns with the findings of Escobar-Ortiz *et al.* [25], who also found that higher temperatures help break cell walls quickly and release solutes. Conversely, the surface remains relatively flat along the time axis, especially at higher temperatures, indicating that extraction reaches equilibrium quickly and extending the process beyond approximately 2 hours adds little extra yield. This pattern agrees with the earlier contour plot and supports the idea that time has a secondary, temperature-dependent effect, as also observed by Ameer *et al.* [26].

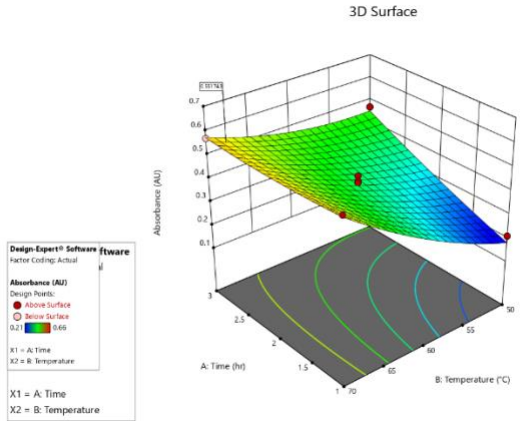

Figure 2. 3D response surface plot showing the effect of time and temperature on absorbance

3.2 Identification of chemical constituents

Phytochemical screening of the F3 fraction from *B. javanica* leaves confirmed the presence of terpenoids, flavonoids, cardiac glycosides, and alkaloids, whereas tannins and saponins were absent (Table 5). This phytochemical profile is consistent with the broader chemical diversity found in the Phyllanthaceae family, where flavonoids, terpenoids, and alkaloids represent significant classes of secondary metabolites. The prominence of flavonoids is particularly noteworthy: a recent review has highlighted that flavonoid and polyphenolic compounds are the dominant classes in many plant-based yellow dyes, owing to their strong light-absorbing conjugated systems [27]. These compounds serve as the chromophoric core in traditional dye plants such as R. *luteola* and continue to play an essential role in contemporary natural dye systems [28].

Although terpenoids are not primary visible chromophores themselves, their hydroxyl, carboxyl, and other polar substituents can function as ligating groups with metal mordants, which enhances dye-fiber binding via coordination complexes [29]. Likewise, cardiac glycosides and alkaloids, while not highly pigmented, may facilitate dye uptake via auxiliary noncovalent interactions (hydrogen bonding and ionic interactions) with protein or cellulosic fiber substrates, thereby aiding in anchoring the primary chromophores within the fiber matrix.

Table 5. Results of the phytochemical screening of *B. javanica* leaves fraction (f3)

Phytochemicals	TLC f3
Terpenoids	+
Tannins	-
Saponin	-
Flavonoids	+
Cardiac Glycoside	+
Alkaloids	+

Key: + Present - Not present

3.3 Spectral and chromatographic evaluation of fraction F3

The absorption maximum at 410 nm shown in Figure 3 is characteristic of yellow flavonoid chromophores. Flavonoids typically exhibit strong Band I absorption between 300 and 380 nm, with the tail of this band extending into the 400-450 nm region, which is responsible for their yellow coloration [30]. This aligns with the observed spectral profile and is further supported by the behavior under $AlCl_3$ complexation, a diagnostic test where measurements in the 410-430 nm range are selective for flavonols and flavones, such as luteolin [31]. The clear, single-band profile with minimal absorption beyond 500 nm confirms the presence of flavonoids and effectively rules out carotenoids or chlorophyll derivatives, which typically display multi-peaked vibronic structures or distinct Q-band features at 600-700 nm, respectively. Similar absorption characteristics have been documented for flavonol-

rich extracts used in natural dyeing applications [32]. The narrow bandwidth points to a predominant chromophore species. It is important to note, however, that dyeing efficiency cannot be assessed solely based on absorbance, as confirmed in previous durability studies

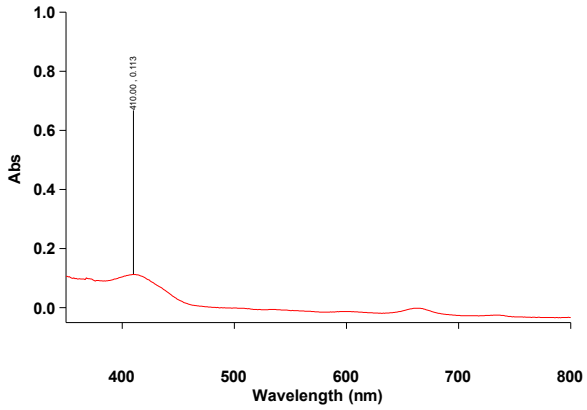

Figure 3. UV-Visible absorption spectrum of Fraction F3 (*B, javanica* leaf dye Extract) from 400-800 nm, showing a dominant peak at 410 nm

This interpretation is strongly corroborated by FTIR analysis (Figure 4). The spectrum shows a broad at 3337 cm^{-1}, indicative of hydrogen-bonded O-H stretches from phenolic groups, and C-H stretching vibrations at 2929 and 2855 cm^{-1}, supporting an aromatic/aliphatic hybrid structure typical of plant secondary metabolites. A particularly diagnostic band at 1610 cm^{-1} corresponds to the conjugated C=C and C=O stretching within the chromen-4-one core, which is highly characteristic of flavones or flavonols. This aligns with the established use of FTIR for flavonoid identification, where key absorptions in the 1650–1400 cm^{-1} range provide critical structural insights [12]. Additional peaks between 1400 and 1000 cm^{-1} are consistent with C-O and C-OH vibrations, which are commonly found in glycosylated phenolic compounds. The absence of strong ester bands (1730–1750 cm^{-1}) and signals associated with porphyrin rings (N-H stretches) effectively rules out significant interference from chlorophyll or non-conjugated ester systems.

.

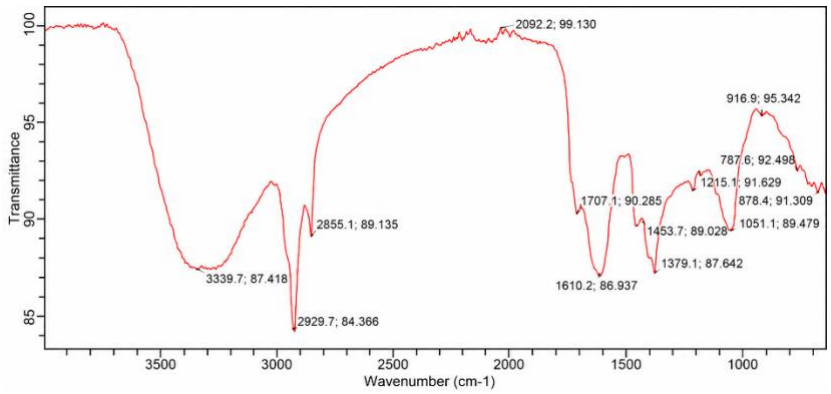

Figure 4. FTIR Spectrum of fraction F3 dye extract (broad O–H stretch at 3339.7 cm^{-1})

These spectroscopic results were corroborated by HPLC profiling, which identified isoquercetin as the primary flavonoid (Rt = 8.081 min) (Figure 5). This identification aligns perfectly with the characteristic UV-Vis maximum at 410 nm and the diagnostic FTIR signature of flavonoid structure. The method also revealed co-occurring compounds: berberine (Rt = 2.498 min) (Figure 6), a yellow chromophore with a distinct UV absorption (340-350 nm), which may synergistically enhance the overall color depth and improve fiber binding through additional ionic and hydrogen-bonding interactions. A minor constituent, eugenol (Rt = 6.005 min) (Figure 7) was also detected, although its specific role in the dyeing process is yet to be fully understood. Collectively, the concordance among UV-Vis, FTIR, and HPLC data establishes the extract as a flavonoid-dominated dye matrix with isoquercetin as the principal chromophore.This identification of a single flavonol glycoside further refines the chemical profile previously reported for the same species by Risnasari *et al.* [5]. Their eco-print study described a broader and less well-defined mixture of polyphenols and lignin-derived compounds rather than an isolated chromophore, highlighting the value of the chromatographic purification approach employed in the present study.

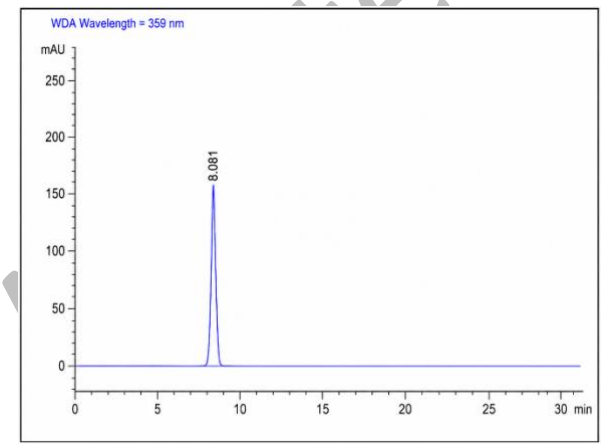

Figure 5. HPLC chromatogram showing a single dominant flavonoid peak at 8.081 min in Fraction F3 (dye extract).

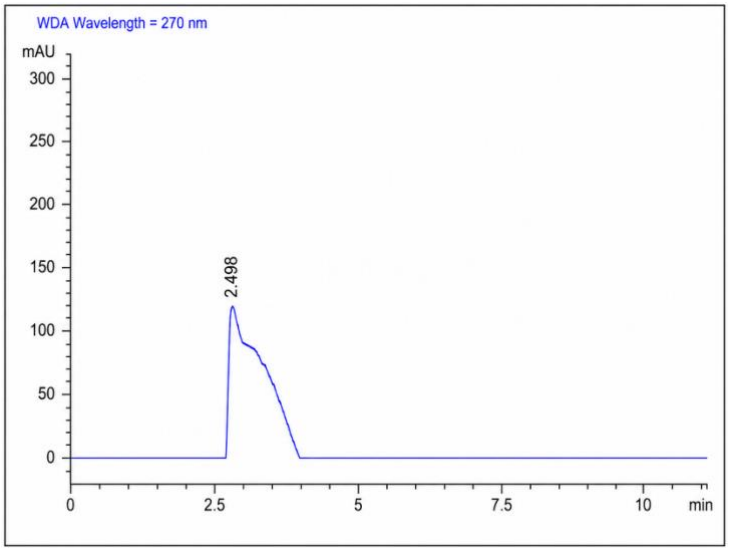

Figure 6. HPLC chromatogram showing a single dominant alkaloid peak at 2.498 min in Fraction F3 (dye extract).

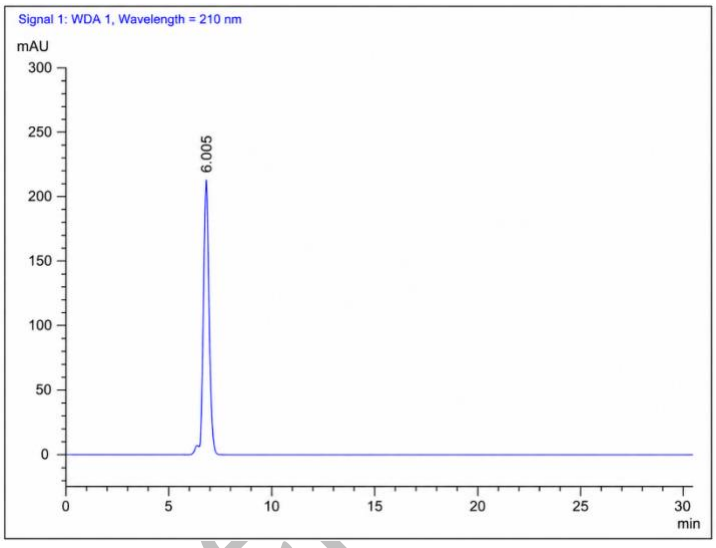

Figure 7. HPLC chromatogram showing a single dominant phenolic peak at 6.005 min in Fraction F3 (dye extract).

3.4 Color fastness properties

Color fastness refers to the ability of a dyed fabric to retain its shade when exposed to light, friction, moisture, or detergent. Since these properties define the functional quality of a textile, the dyed samples were tested for wash, perspiration, rubbing, and light fastness.

3.4.1 Wash fastness

Wash fastness results (Table 6, Figure 8) show that mordanting considerably improves dye retention at low concentrations (2–4%). Aluminum ions from $KAl(SO_4)_2$ coordinate with the hydroxyl groups of flavonoid chromophores, forming stable metal–dye–fiber complexes. In contrast, unmordanted fabrics depend only on weak

hydrogen bonding and van der Waals interactions, resulting in greater dye loss during washing. This result is in accordance with that of Clark and Ekpekpo [10], who demonstrated that metal–dye complexes create more stable linkages with cellulosic fibers than unmordanted samples relying on hydrogen bonding alone.

However, the effect of mordanting on staining becomes less pronounced at higher dye concentrations (6–8%). Once the available coordination sites on cotton are saturated, excess dye remains physically adsorbed on the fiber surface regardless of the mordant. This loosely bound dye is easily removed during washing, leading to comparable staining grades for the mordanted and unmordanted samples despite superior overall fixation in the treated fabrics.

Table 6. Wash fastness of *B. javanica* leaves

		Mordanted ($KAl(SO_4)_2$)		Unmordanted	
S/NO	Samples	Color change	Staining	Color change	Staining
1	BJ 2%	3-4		2-3	3
2	BJ 4%	3	3	2	2-3
3	BJ 6%	3	2	2	2
4	BJ 8%	4	3	2-3	2-3

Key: BJ-dye concentration, 1-poor, 2-fair, 3-good. 4-very good. 5-excellent

3.4.2 Light fastness

The light fastness evaluation (Table 7, Figure 8) demonstrates the significant photostabilizing effect of mordanting. At 2% dye concentration, the mordanted fabric achieved grade 5, while the unmordanted sample remained at grade 3, indicating marked fading. This enhanced stability arises from the coordination of Al^{3+} ions with flavonoid chromophores, which stabilizes their excited states after photon absorption and facilitates non-radiative relaxation. The resulting metal-dye complexes reduce oxidative photodegradation by quenching singlet oxygen and minimizing reactive oxygen species.

At 4–6% dye levels, both fabric types showed improved resistance owing to increased dye loading, which distributes photon exposure across more molecules. Nevertheless, the mordanted samples consistently retained higher grades (5–6 to 6) compared to unmordanted fabrics (4-5), confirming that chemical stabilization rather than simple concentration effects is responsible for the superior performance.

At 8%, mordanted cotton reached grade 6-7, approaching the light-fastness range of synthetic dyes. The unmordanted fabric improved to grade 5-6 due to self-shading effects from dense dye accumulation, yet it still performed below that of the mordanted cotton. This confirms that although a higher dye concentration offers passive protection, aluminum-flavonoid coordination remains the dominant mechanism governing long-term photostability, as demonstrated by Haar *et al.* [33], who reported that metal mordanting significantly enhances light fastness of natural dyes to commercially acceptable levels.

Table 7. Light fastness of *B. javanica* leaves

		Mordanted ($KAl(SO_4)_2$)	Unmordanted
S/NO	Samples	Grades	Acid
1	BJ 2%	5	3
2	BJ 4%	5-6	4-5
3	BJ 6%	6	4
4	BJ 8%	6-7	5-6

Key: BJ-dye concentration, 1-very poor, 2-poor, 3-fair. 4-moderate. 5-good, 6-very good, 7-excellent, 8-outstanding

3.4.3 Perspiration fastness

Perspiration fastness (Table 8, Figure 8) revealed a more complex mordanting response compared to wash or light fastness. Under acidic conditions (pH 5.5), both mordanted and unmordanted samples displayed good stability at 2% concentration (grades 4 and 3-4, respectively). The small difference suggests that protonation of phenolic groups does not significantly disrupt dye-fiber interactions; in fact, acidic pH may reinforce hydrogen bonding between protonated flavonoids and cellulose. The modest advantage of the mordanted cotton reflects additional anchoring from Al^{3+} coordination. Under alkaline perspiration (pH 8), fastness dropped sharply, even at low dye levels (mordanted: grade 3; unmordanted: 2–3), consistent with earlier reports that alkaline sweat destabilizes metal–dye complexes through deprotonation of OH groups and potential $Al(OH)_3$ precipitation. This leads to dye solubilization as phenolate anions. At 4–6% dye concentration, performance declines further, especially in mordanted samples, as loosely bound dye accumulates beyond available coordination sites and becomes easily extracted. The lowest values occur at 6%, indicating a saturation threshold where surface-deposited dye dominates the response rather than coordinated dye. The slight recovery at 8% aligns with that reported by Rehman *et al.* [34], who reported that very high dye loadings can improve fiber penetration and mechanical entrapment, providing modest protection even when chemical bonding sites are exhausted. Clark *et al.,* [35] further confirmed that alkaline perspiration remains the most challenging fastness test for natural dyes, even with optimal mordanting protocols. In practical terms, the poor performance under alkaline conditions narrows the practical applications of the dye rather than negating them. Textiles intended for prolonged exposure to alkaline perspiration or high-pH laundering, such as sportswear, undergarments, and workwear, would be most affected, whereas decorative, furnishing, and craft fabrics, as well as garments laundered under neutral to mildly acidic conditions, remain within an acceptable performance range. The observed behavior could potentially be improved by replacing or supplementing the alum mordant with iron- or tannin-based biomordants that form less pH-sensitive complexes, applying a cationic fixing agent or back-tanning treatment to enhance chromophore retention within the fiber, or buffering the finished textile towards neutrality. Each of these approaches warrants systematic investigation before large-scale application.

Table 8. Perspiration fastness of *B. javanica* leaves

		Mordanted ($KAl(SO_4)_2$)		Unmordanted	
S/NO	Samples	Acid	Alkaline	Acid	Alkaline
1	BJ 2%	4	3	3-4	2-3
2	BJ 4%	3-4	3	3	2-3
3	BJ 6%	2-3	2	2	1-2
4	BJ 8%	3	3	2-3	2

Key: BJ-dye concentration, 1-poor, 2-fair, 3-good. 4-very good. 5-excellent

3.4.4 Rubbing fastness

The rubbing fastness results (Table 9, Figure 8) revealed less pronounced differences between the mordanted and unmordanted fabrics compared to the other fastness properties.

At low dye concentrations (2%), mordanted fabrics show improved rubbing fastness compared to unmordanted fabrics, particularly in wet conditions. This is because mordants chemically fix the dye molecules to the fabric, reducing the mobile unfixed dye fraction that can migrate during wet rubbing, as noted in studies where mordants, such as potassium aluminum sulfate, improve wet and dry rubbing fastness. The chemically fixed dye fraction in mordanted fabrics resists displacement in the presence of moisture, which otherwise promotes dye transfer in unmordanted fabrics [35].

The observed decrease in rubbing fastness at higher dye concentrations (4% and above) also matches the reported findings. At elevated dye loading, an excess of loosely bound or surface-accumulated dye increases the likelihood of mechanical removal during rubbing, which diminishes both wet and dry fastness grades. Even mordanted fabrics can have loosely bound dye at these levels, explaining the convergence of fastness grades between mordanted and unmordanted samples as dye concentration increases [36].

The stable dry rubbing grades (around 4) at higher concentrations reflect that dry friction is less effective at

mobilizing dye physically entangled within the fiber matrix, regardless of the presence of the mordant. This observation is consistent with literature noting that physical entrapment and absence of moisture reduce dye migration under dry rubbing.

Table 9. Rubbing fastness of *B. javanica* leaves

		Mordanted ($KAl(SO_4)_2$)		Unmordanted	
S/NO	Samples	Wet	Dry	Wet	Dry
1	BJ 2%	4	3	3	2-3
2	BJ 4%	3	2-3	2-3	2
3	BJ 6%	3-4	4	3	3-4
4	BJ 8%	3	4	2-3	3-4

Key: BJ-dye concentration, 1-poor, 2-fair, 3-good. 4-very good. 5-excellent

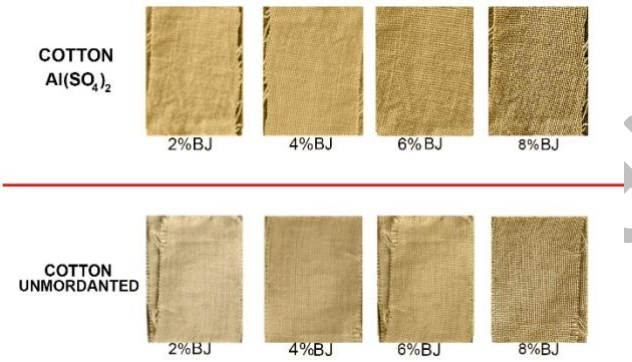

Figure 8. Cotton fabrics dyed with fraction F3

Table 10. Color coordinate values and color strengths of cotton samples mordanted with $KAl(SO_4)_2$ and dyed with fraction F3 from *B. javanica* leaves

Sample	Concentration of mordant %	K/S	L*	a*	b*	C*	H*
Non-mordanted Cotton	-	2.8	48.2	2.9	4.7	11.2	50.4
$KAl(SO_4)_2$	2	4.6	36.8	4.9	6.1	13.4	51.7
	4	6.1	35.1	5.6	7.4	14.8	52.9
	6	7.9	33.9	6.4	8.5	16.3	53.8
	8	9.1	31.4	4.7	9.1	17.6	62.1

Key: K/S- Strength of the shade of dyed sample, L* Brightness, a* Extent of redness, b* Extent of yellowness or blueness, H-Hue angle

3.4.5 Color measurement

Table 7 presents the changes in the K/S values for both mordanted and unmordanted cotton samples at varying concentrations. Consistent with previous studies on the mordant effects in textile dyeing, untreated cotton displayed the lowest color strength (K/S = 2.8) and the highest lightness (L* = 48.2), reflecting a pale and muted

color. When mordanted with potassium aluminum sulfate, there was a clear, concentration-dependent increase in dye absorption. At 2% mordant, the K/S value increased to 4.6, showing moderate darkening, while higher concentrations of 4% and 6% further elevated K/S to 6.1 and 7.9, respectively. This trend aligns with existing reports that highlight the role of mordants in enhancing dye–fiber interactions. The maximum concentration of 8% produced the deepest coloration with a K/S of 9.1 and a substantial reduction in L* (31.4), indicating a richer and darker shade. Moreover, chroma (C*) values progressively rose from 11.2 to 17.6, suggesting improved color saturation, while hue angle (H*) exhibited a slight shift at 8%, moving toward warmer yellow tones. These findings agree with prior research demonstrating that potassium aluminum sulfate not only intensifies color depth but also affects tonal qualities.

4. CONCLUSION

This study successfully demonstrates that combining Soxhlet extraction with RSM-CCD is a highly effective strategy for optimizing the natural dye yield from *Bischofia javanica* leaves, achieving a threefold increase under the determined optimal conditions of 70 °C for 2 hours. The main colorant was identified and purified as flavonoid isoquercetin. When applied to cotton using a potassium aluminum sulfate mordant, the dye produced a shade with significantly enhanced color strength (K/S). The mordanted fabric exhibited excellent fastness properties (grade 6–7) and very good wash and dry rubbing fastness (grade 4) at 8% dye concentration. A key finding was the superior fastness under acidic perspiration, which is attributed to the formation of stable aluminum-flavonoid complexes, emphasing the critical role of mordant-dye chemistry. These results firmly establish *Bischofia javanica* leaves as a viable and promising source of natural dyes for sustainable textiles. However, reduced colour stability under alkaline conditions remains a limitation, and future studies should explore strategies to improve alkaline fastness and evaluate the dye's performance on other textile fibres, particularly wool and silk.

REFERENCES

1. P. D. Clark, J. O. Otutu, K. A. Asiagwu, G. I. Ndukwe, and C. A. Idibie, Investigating the feasibility of utilizing *Pennisetum purpureum* leaves waste as a sustainable dye: Etraction, characterization and application on textile, *Sci. Afric.,* **2023**, 22 (3), 231-246.
2. D. Ardila-Leal, R. A. Poutou-Piñales, A. M. Pedroza-Rodríguez, and B. E. Quevedo-Hidalgo, A brief history of colour, the environmental impact of synthetic dyes and removal by using laccases, Molecules, **2021**, 26 (13), 2-40.
3. S. Lee, A. J. H, J. Park, E. Kang, S.-H. Jeon, S. B. Han, S. Ningsih, J. H. Paik, and S. Cho, Antioxidant and anti-inflammatory effects of *Bischofia javanica* (Blume) leaf methanol extracts through the regulation of Nrf2 and TAK1, Antioxidants, **2021**, 10(8), 2-18.
4. J. Gao, Y. Zhao, F. Ni, M. Gao, L. Wu, Z. Yu, Y. Chen, and Y. Wang, Polyphenol metabolomics reveals the applications and prospects of polyphenol-rich plants in natural dyes, Forestry Research, **2024**, 4, e035.

5. I. Risnasari, N. N. Solihat, R. Rambey, R. Purnawati, M. Ismayati, and F. P. Sari et al., Characterization and application of Sikkam (*Bischofia javanica* Blume) as a natural dye and antibacterial agent for eco-printing textiles, Waste Biomass Valor, **2025**, 16, 4863-4878.
6. S. Jabeen, S. Ali, M. Nadeem, K. Arif, N. Qureshi, G. A. Shar, G. A. Soomro, M. Iqbal, A. Nazir, and U. H. Siddiqua, Statistical modeling for the extraction of dye from natural source and industrial applications, *Pol J Environ Stud*, **2019**, 28(4), 2145-2150.
7. N. Amin, F.-U. Rehman, S. Adeel, M. Ibrahim, and R. Mia, Eco-friendly extraction and utilization of agro crop wastes based natural dye for textile dyeing, Energy Sci Eng, **2025**, 13(1), e2067.
8. V. Rotich, P. Wangila, and J. Cherutoi, FT-IR analysis of *Beta vulgaris* peels and pomace dye extracts and surface analysis of optimally dyed-mordanted cellulosic fabrics, J Chem, **2022**, 2022(1), 2233414.
9. V. Popescu, A. C. Blaga, M. Pruneanu, I. N. Cristian, M. Pisiaru, A. Popescu, V. Rotaru, I. Cretescu and D. Cascaval, Green chemistry in the extraction of natural dyes from colored food waste, for dyeing protein textile materials, *Polymers*, **2021**, 13(22), 3867.
10. P. D. Clark and L. D. Ekpekpo, Maceration-based extraction and spectroscopic characterisation of *Sorghum bicolor* leaves extract as a natural dye on cotton fabric, *J Chem Soc Nigeria*, **2025**, 50(4), 775-786.
11. J. O. Otutu, P. D. Clark, M. E. Osharode, E. C. Otutu, and G. I. Ndukwe, Extraction, characterization, and application of a polyphenolic compound as a natural dye for polyamide fabrics, *J Chem Lett, vol.,* **2025**, 6, 68-78.
12. P. D. Clark, J. O. Otutu, K. A. Asiagwu, G. I. Ndukwe, E. C. Otutu, and C. A. Idibie, Isolation and characterization of natural dyes from *Persea americana* leaves and their application on polyamide fabrics, *Ovidius Univ Ann Chem.,* 2025, 36(2), 91-102.
13. G. I. Ndukwe, J. G. Tetam, and P. D. Clark, Phytochemical screening and *in vitro* antioxidant assessment of *Cassia alata* (Linn) leaf extracts, *ChemSearch J*., **2020**, 11(2), 64-72.
14. G. I. Ndukwe, P. D. Clark, and I. R. Jack, *In vitro* antioxidant and antimicrobial potentials of three extracts of *Amaranthus hybridus* L. leaf and their phytochemicals, *Eur Chem Bull.*, **2020**, 9(7), 164-173.
15. P. D. Clark and E. Omo-Udoyo, A comparative assessment on antioxidant and phytochemical of *Trichilia monadelpha* (Thonn) J.J. De Wilde (Meliaceae) plant extracts, *Chem Sci Int J*., **2021**, 30(10), 24-33.

16. ISO 105-C10:2006 Textiles: Tests for colour fastness. Part C10. Colour fastness to washing, ISO, Basel, 2006.
17. ISO 105-B01:2014 Textiles: Tests for colour fastness. Part B01. Colour fastness to light, ISO, Basel, 2014.
18. ISO 105-X12:2013 Textiles: Tests for colour fastness. Part X12. Colour fastness to rubbing, ISO, Basel, 2013.
19. ISO 105-E04:2013 Textiles: Tests for colour fastness. Part E04. Colour fastness to perspiration, ISO, Basel, 2013.
20. C. E. Ochoa-Velasco and I. I. Ruiz-López, Mass transfer modeling of the antioxidant extraction of roselle flower (*Hibiscus sabdariffa*), *J Food Sci Technol*., 2019, 56(2), 1008–1015
21. Q. W. Zhang, L. G. Lin, and W. C. Ye, Techniques for extraction and solation of natural products: A comprehensive review, *Chin Med.,* **2018**, 13(20), 2-26.
22. S. Carpentieri, G. Ferrari, and G. Pataro, Optimization of pulsed electric fields-assisted extraction of phenolic compounds from white grape pomace using response surface methodology, *Front Sustain Food Syst*., **2022**, 6, 854968.
23. I. S. C. Sulaiman, M. Basri, H. R. Fard Masoumi, W. J. Chee, S. E. Ashari, and M. Ismail, Effects of temperature, time, and solvent ratio on the extraction of phenolic compounds and the anti-radical activity of *Clinacanthus nutans* Lindau leaves by response surface methodology, *BMC Chem*., **2017**, 11, 2-11.
24. A. Antony and M. Farid, Effect of temperatures on polyphenols during extraction, *Appl Sci*., **2022**, 12 (4), 2107.
25. M. Cano-Lamadrid, L. Martínez-Zamora, L. Mozafari, M. C. Bueso, M. Kessler, and F. Artés-Hernández, Response surface methodology to optimize the extraction of carotenoids from horticultural by-products: A systematic review, *Foods*., **2023**, 12 (24), 4456.
26. A. Escobar-Ortiz, Y. Salinas-Moreno, J. Jiménez-Hernández, and J. A. Gutierrez-Uribe, Effect of extraction temperature on anthocyanin yield and stability from *Hibiscus calyx*, *Ind Crops Prod*., **2021**, 171, 113916.
27. K. Ameer, H. M. Shahbaz, J. H. Kwon, and Y. Jo, Green extraction methods for polyphenols from plant matrices and their byproducts: A review, *Compr Rev Food Sci Food Saf*., **2017**, 16(2), 295-315.

28. S. Yadav, K. S. Tiwari, C. Gupta, M. K. Tiwari, A. Khan, and S. P. Sonkar, A brief review on natural dyes, pigments: Recent advances and future perspectives, **2023**, *Results Chem*., 5, 100733.
29. E. O. Alegbe and T. O. Uthman, A review of history, properties, classification, applications and challenges of natural and synthetic dyes, *Heliyon*, **2024**, 10(13), 33646.
30. H. Benli, Bio-mordants: A review, *Environ Sci Pollut Res.,* **2024**, 31, 20714-20771.
31. M. Taniguchi, C. A. Larocca, J. D. Bernat, and J. S. Lindsey, Digital database of absorption spectra of diverse flavonoids enables structural comparisons and quantitative evaluations, *J Nat Prod*., **2023**, 86 (4), 1087-1119.
32. A. Pękal and K. Pyrzynska, Evaluation of aluminium complexation reaction for flavonoid content assay, *Food Anal Methods*., **2014**, 7(8), 1776-1782.
33. S. Haar, E. Schrader, and B. M. Gatewood, Comparison of aluminum mordants on the colorfastness of natural dyes on cotton, *Clothing and Textiles Research Journal,* **2013**, 31(2), 97-108.
34. A. Rehman, M. Irfan, A. Hameed, M. J. Saif, M. A. Qayyum, and T. Farooq, Chemical-free dyeing of cotton with functional natural dye: A pollution-free and cleaner production approach, *Front Environ Sci*., **2022**, 10, 848245.
35. P. D. Clark, J. O. Otutu, K. A. Asiagwu, and G. I. Ndukwe, Exploring the potential of *Dacryodes edulis* leaf extract as natural colourant on polyamide fabrics: Extraction, characterization and application, *Substantia*, **2024**, 8(2), 103-118.
36. G. Ramratan and J. Rani, Optimization rubbing fastness in Lyocell and silk fabric dyeing with *Tinospora cordifolia* using Box-Behnken design and *Citrus limon* extract with potassium aluminium sulfate mordants, *Text Leather Rev.*, **2023**, 6, 475-497.